

Facile Graphene Oxide Preparation by Microwave-Assisted Acid Method

Marcelo M. Viana,^{*a} Meiriane C. F. S. Lima,^b Jerimiah C. Forsythe,^c Varun S. Gangoli,^c
Minjung Cho,^c Yinhong Cheng,^c Glaura G. Silva,^b Michael S. Wong^c and
Vinicius Caliman^b

^aDepartamento de Física e Química, Instituto de Ciências Exatas e Informática,
Pontifícia Universidade Católica de Minas Gerais, 30535-901 Belo Horizonte-MG, Brazil

^bDepartamento de Química, Instituto de Ciências Exatas, Universidade Federal de Minas Gerais,
31270-901 Belo Horizonte-MG, Brazil

^cDepartment of Chemical and Biomolecular Engineering, Rice University, 77005 Houston-TX, USA

Few-layered graphene oxide (GO) was prepared using a fast and energy-saving method by microwave-assisted acid technique. The oxygenated groups existing on the GO surface were determined using UV-Vis, X-ray photoelectron and Fourier-transform infrared spectroscopies. An oxygenated group percentage of 30% in mass for the GO was observed by thermogravimetric analysis. The reduced few-layered graphene oxide (rGO) film annealed at 110 °C deposited onto a silicon/silica wafer showed expanded graphite-like structure with 0.70 nm between the rGO sheets, as determined by X-ray diffraction. This rGO film exhibited a relatively high electrical conductivity value of $7.36 \times 10^2 \text{ S m}^{-1}$ confirming the good restoration of the π -conjugated system. The prepared GO sample exhibited good stability in water from pH 4 to 12, as determined by its zeta potential, and contained 5 to 9 layers, as determined by atomic force microscopy (AFM) and transmission electron microscopy (TEM).

Keywords: microwave irradiation, graphene oxide, film, conductivity

Introduction

Scientific and technological progress involving the preparation and application of graphene since its preparation from micromechanical exfoliation by Novoselov *et al.* in 2004¹ has necessitated the development of several methodologies for its production from graphite: a top-down process. Some chemical routes lead to the preparation of graphene oxide (GO), which is a single layer of carbon atoms that contains both C–C and C–O bonds with sp^2 and sp^3 hybridization and which is considered a new type of non-stoichiometric macromolecule that is chemically labile and hygroscopic under ambient conditions.² GO has been mainly prepared using methods based on the original studies of Brodie,³ Staudenmaier⁴ and Hummers and Offeman,⁵ which involve oxidation of the graphite structure. The Hummers method is an efficient and widely used approach to prepare GO nanosheets, i.e., few-layered GO; however, considerable time is required to prepare GO

in this manner. Some alternative chemical methods have also been used, such as solvothermal,⁶ electrochemical⁷ and microwave-assisted methods,⁸⁻¹⁰ which are rapid and efficient approaches to exfoliating graphite.

Structural models of GO have been developed in some studies¹¹⁻¹⁴ because GO is used as an intermediate material in the preparation of reduced GO (rGO); however, the structure of GO has not been fully elucidated. Some questions involving the hexagonal lattice, planarity, the binding of the oxygen to the carbon and the acid properties in aqueous solutions remain open. Recently, some important progress has been achieved in GO-related structural studies involving high-resolution transmission electron microscopy (HRTEM) and the Boehm titration protocol.^{15,16} The structural configuration of GO after chemical treatments is dependent on the preparation method, which can result in, for example, paper-like GO, a material with exciting mechanical properties that was first prepared by Dikin *et al.*¹⁷

The oxygenated groups present in GO contribute to its dispersibility in polar media, e.g., water, and also facilitate non-covalent and covalent modification, which

*e-mail: marcelopuc.viana@yahoo.com.br

enables the development of graphene-based materials. The oxidation process also contributes to a reduction in the electrical conductivity compared with that of pristine graphene because of the formation of defects and disorders in the graphene structure.¹⁸ Chemical reduction reactions performed on GO can partially restore the conductivity of the GO sheets, leading to rGO that is suitable for use in various applications.^{18,19} Various scientists have attempted different chemical methods to prepare GO using processes that conserve reactants, time and energy.²⁰ For example, Wan *et al.*²¹ proposed an energy-saving freeze-dried method to prepare rGO which demonstrated great application potential for electrical energy storage.

In this work, we report a fast and reproducible process to prepare GO from graphite using microwave (MW) irradiation under acidic conditions. The GO sheets and rGO film were characterized mainly by ultraviolet-visible spectroscopy (UV-Vis), transmission electron microscopy (TEM), atomic force microscopy (AFM), thermogravimetric analysis (TGA), X-ray diffraction (XRD), Fourier-transform infrared spectroscopy (FTIR), scanning electron microscopy (SEM), X-ray photoelectron spectroscopy (XPS), and electrical measurements.

Experimental

Materials

Graphite was purchased from Bay Carbon (SP-1, grade 325 mesh). Nitric acid (HNO₃), sulfuric acid (H₂SO₄), potassium permanganate (KMnO₄), hydrogen peroxide (H₂O₂), and hydrochloric acid (HCl) were purchased from Sigma-Aldrich. All of the materials were used as received, and the solutions used in the experiments were prepared with deionized water.

GO preparation

Natural graphite powder, 70% nitric acid and KMnO₄ were mixed in a graphite:HNO₃:KMnO₄ weight ratio of 1:2:1,⁹ and the resulting mixture was magnetically stirred in a glass flask for 10 min at room temperature. The acid dispersion was transferred to a crucible, and the dispersion was irradiated in a domestic Emerson microwave at 900 W for 60 s. The powder obtained was then rinsed with deionized water until pH 7 and dried at 110 °C for 3 h to yield expanded graphite (EG). The oxidation and exfoliation were conducted as described: 2.2 mL of H₂SO₄ and 1.0 g of KMnO₄ were added to 1.0 g of EG and the mixture was magnetically stirred for 30 min to produce a green dispersion. Deionized water was subsequently added,

and this dispersion was sonicated for 2 h, causing its color change to brown. Subsequently, 10 mL of 30% H₂O₂ was slowly added to the dispersion, and the color changed from brown to bright-yellow. This mixture was washed with 10% HCl and deionized water until neutral. The brown washed powder, which was precipitated GO, was dried at 110 °C overnight, and a graphene oxide film (rGO) was formed after the water was evaporated. The total time required to prepare the GO film was 24 h.

Characterization

UV-Vis absorbance spectroscopy performed on a Shimadzu UV-Vis (UV-24601 PC) spectrophotometer was used to evaluate the stability of the GO aqueous dispersion. The photoluminescence (PL) of the GO sheets in aqueous solution was measured using a Jobin Yvon Fluoromax-3 fluorimeter. The sample was excited at a wavelength of 480 nm to collect its emission in the 500-800 nm range. The PL intensity was determined by integrating the PL peak.

The zeta potential of the GO sheets was determined on a Brookhaven Zeta PALS instrument.

HRTEM micrographs were obtained using an JEOL 2100F FEG-TEM operated at 200 kV using holey-carbon-coated copper grids. SEM was performed on an ESEM FEG FEI Quanta 400.

TGA was performed on a TA Q50 instrument at a heating rate of 1 °C min⁻¹ from room temperature to 800 °C. The experiment was performed under an argon atmosphere flowing at 20.0 mL min⁻¹. Differential scanning calorimetry (DSC) measurements were performed on a 2920 model calorimeter from TA Instruments.

X-ray diffraction (XRD) measurements were performed on a Rigaku D/Max 2550 diffractometer equipped with a CuK_α radiation source ($\lambda = 1.5418 \text{ \AA}$).

FTIR spectra were recorded on a Nicolet attenuated total reflectance Fourier transform infrared spectroscopy (ATR-FTIR) spectrophotometer in transmission mode (128 scans and resolution of 4 cm⁻¹).

Atomic force microscopy (AFM) images were obtained on a Asylum Research MFP-3D-SA SPM microscope under ambient conditions. AFM was performed in tapping mode using an Olympus AC240TS silicon cantilevers with a spring constant of 2.0 N m⁻¹.

XPS measurements were performed in a PHI QUANTERA Physical Electronics XPS/ESCA system. A monochromatic Al X-ray source operated at 100 W was used with a pass energy of 26 eV and a 45° take-off angle. Low-resolution survey scans and higher-resolution scans of C and O were performed.

Electrical measurements were performed on rGO film formed by drop-casting the GO dispersion onto Si/SiO₂ wafers and subsequently annealing the coated wafer in air at 110 °C overnight. The surface resistivity was measured using a Lakeshore CPX four-point probe at room temperature.

Results and Discussion

The 1-day GO film preparation method proposed here is a fast method compared to some reported methods used to prepare GO nanosheets.^{17,22,23} Comparing to the literature,^{24,25} it involves a simple and quick purification process which eliminates the more oxidized GO sheets to give a high conductivity film after the annealing process.

Figure 1 illustrates the 4 steps involved in the preparation of the rGO film, which are mainly: (1) expansion, (2) oxidation and exfoliation, (3) purification and (4) annealing. The graphite expansion (step 1) under MW radiation is accompanied by fuming and lightening, with formation of gases that promote violent expansion along the c-axis to yield graphite worms, i.e., expanded graphite (EG). Step 2 involves the acid sonication of the EG to obtain GO sheets. During the washing and centrifugation process, the color gradually darkens (Figure 1, step 3), suggesting that larger sheets are present and that the π -system conjugation has expanded.²⁶ As the water evaporates during the drying process, the sheet-to-sheet van der Waals interactions become more effective and the GO sheets self-assemble leading to aggregates that will deposit as a film. The uniformity and thickness of the formed rGO film (Figure 1, step 4) and the color, which can vary from brown to black, are dependent on the amount of graphite used in the starting process.

Firstly we characterized the GO in an aqueous dispersion using UV-Vis spectra which exhibited a characteristic maximum absorption at 230 nm, as observed in Figure 2a; this maximum is assigned to the π -to- π^* transition of C=C bonds, and the broad shoulder between

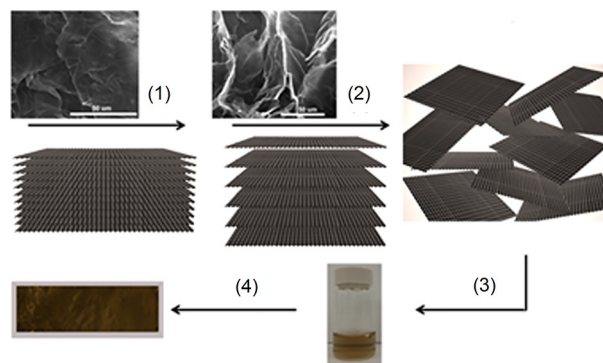


Figure 1. Chemical route to prepare a rGO film. Steps: (1): expansion of graphite to prepare expanded graphite (EG) using HNO₃:KMnO₄ and 900 W MW radiation; (2): oxidation and exfoliation of EG in H₂SO₄/KMnO₄ solution by sonication; (3): the GO dispersion formed after the EG has been rinsed with deionized water (pH 6); and (4): the rGO film formed after drying at 110 °C.

290-300 nm is assigned as the n-to- π^* transition of C=O bonds.²⁷ Over a period of 30 days, the concentration of GO in the suspension decreased by approximately 12% due to some precipitation, and no shift was observed in the absorption maximum. A PL peak at 545 nm was attributed to electron-hole recombination between conduction band and neighbor-localized states to valence band. The oxidized and non-oxidized carbon on GO are responsible for emission species to visible fluorescence.²⁸

Zeta-potential measurements were performed on as-prepared GO aqueous nanofluids at different pH values. The results are presented in Figure 2b. We observed a negative charge on the GO surface on the full pH scale; in addition, at pH levels ranging from 4 to 12, the GO nanofluids exhibited considerable stability. According to ASTM definitions,²⁹ aqueous colloidal systems with zeta potentials more negative than -40 mV exhibit good stability. However different publications^{27,30} have considered a zeta potential more negative than -30 mV sufficient for a stable GO dispersion. They also have shown the tendency in the zeta potential toward positive values under highly acidic conditions due to protonation of different groups (carboxylic or/and hydroxyl group) present at the GO surface.

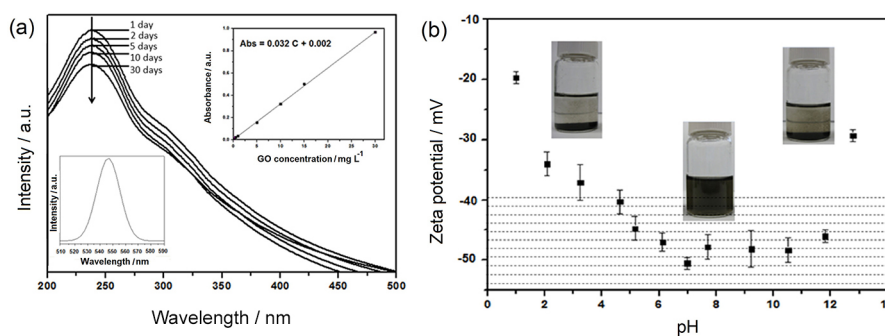


Figure 2. UV-Vis spectra of GO nanosheets dissolved in water for 30 days in (a). The inset (top) shows the linear relationship between the absorbance and the GO concentration; the inset (bottom) shows the normalized PL spectrum. Zeta potential measurements of a 0.25 mg mL⁻¹ GO sample in water in (b).

The GO sheets were imaged by TEM before being dried to form the rGO film. Figures 3a and 3b show the presence of mostly few-layered and folding GO sheets with lateral dimensions ranging from 1 to 10 μm .

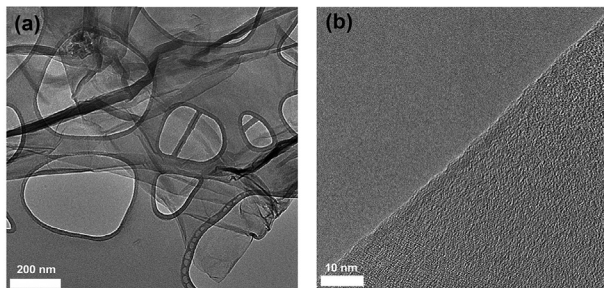


Figure 3. (a) TEM of GO and (b) HRTEM of few-layered GO nanosheets.

The AFM images of the GO sample (Figure 4) easily confirm the wrinkled 2D characteristic of the GO sheets; the images indicate that the thicknesses of both samples were approximately 1.5 to 3.0 nm, corresponding to structures with 5 to 9 layers.

On sequence are presented the characterizations of rGO film. TGA/DTG curves (Figure 5a) reveal two well-defined steps of mass loss. The first step, which involves a 15% mass loss at a maximum temperature of 100 $^{\circ}\text{C}$, corresponds to the elimination of water and volatile molecules. Between 100 $^{\circ}\text{C}$ and 250 $^{\circ}\text{C}$, the film lost an additional 30% mass

related to oxygenated groups present in the rGO film. The continuous mass loss corresponds to pyrolysis of the carbon structure of the rGO film.³¹

The expansion effect on the graphite structure due to hydration and oxygen-group intercalation was evaluated by XRD. Figure 5b shows the pristine graphite main peak (002) centered at 26.6 $^{\circ}$, which corresponds to an interlayer distance d_{002} of 0.33 nm.³² We also prepared a flat and homogeneous film using the rGO sheets formed after chemical treatments to perform structural and electrical measurements. The sheets were deposited onto Si/SiO₂ substrates and dried in air at 110 $^{\circ}\text{C}$ overnight. In this film, the graphite peak at 26.6 $^{\circ}$ is broader than that characteristic of pristine graphite, suggesting an increase in structural disorder and in the size distribution of the rGO sheets.³² The relatively intense peak (002) suggest that during annealing process some rGO sheets were re-stacked forming a graphite-like structure. After the annealing process, the graphite main peak at 26.6 $^{\circ}$ is not observed and the peak at 12.7 $^{\circ}$, which corresponds to an interlayer distance of 0.70 nm, provides evidence of GO exfoliation. When the rGO film was formed on drying the water dispersion, the 12.7 $^{\circ}$ peak became more prominent, whereas the peak at 26.6 $^{\circ}$ peak vanished, indicating that the film was formed by an expanded graphite-like structure with a distance of 0.70 nm between the rGO sheets.¹⁵ The broadening of this peak indicates a smaller sheet size compared to those of

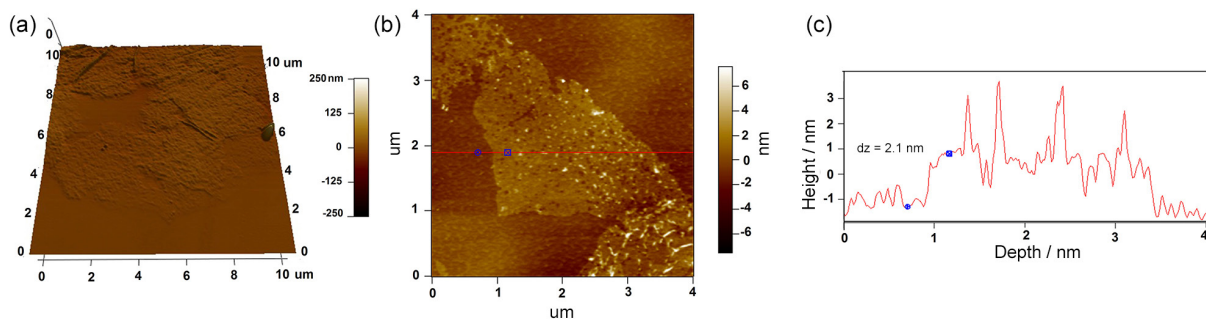


Figure 4. (a) 3D AFM images of GO; (b) 2D images and (c) profile showing the approximately 6 sheets of graphene.

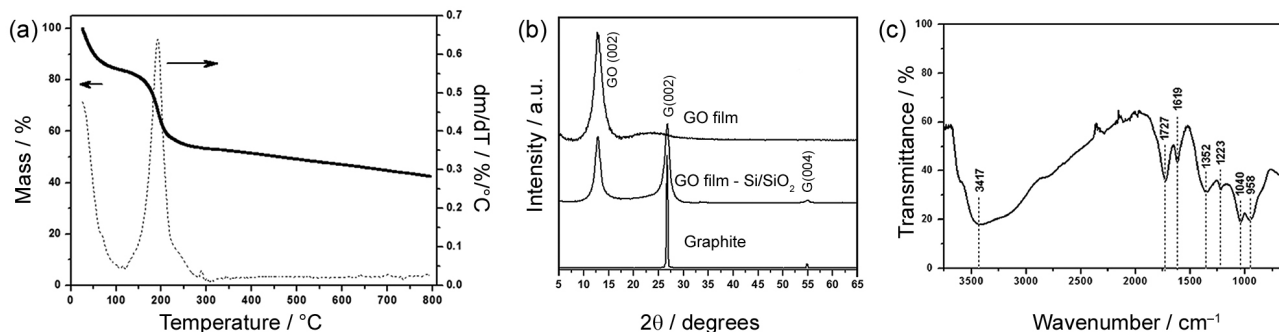


Figure 5. (a) TGA/DTG curve of a rGO film under an argon atmosphere. (b) XRD profiles of graphite, a rGO film deposited onto a Si/SiO₂ substrate and a rGO film annealed at 110 $^{\circ}\text{C}$ overnight. (c) ATR-FTIR spectrum of the rGO film.

the original graphite powder and the rGO film deposited onto Si/SiO₂.

The ATR-FTIR spectrum of the rGO film recorded in the range of 4000-450 cm⁻¹ is presented in Figure 5c. The characteristic bands observed in this spectrum (Table 1) confirm the functional groups present in the structure of the rGO film. The efficiency of the oxidizing process can be confirmed mainly by the absorption bands at 1727 cm⁻¹ (C=O stretching vibration) and 1352 cm⁻¹ (C-O-H deformation of the carboxylic acid).³¹

Table 1. IR frequencies and corresponding functional groups of the rGO film

IR frequency / cm ⁻¹	Bond and functional group
3417	O-H stretching vibration
1727	C=O stretching vibration
1619	Water-bending modes
1352	O-H deformation
1223	C-OH stretching vibration
1040	Epoxy C-O vibration
958	O-H out-of-plane vibration

Figures 6a and 6b present SEM images of the prepared rGO film. Figure 6a shows the morphology of the surface resulting from considerable folding of an individual rGO sheet. Figure 6b shows the fracture edge of a rGO film with

a thickness of 30 μm. The rGO film contained sandwiched, well-packed layers with some cracks that were most likely formed by water evaporation during drying.

Topography and phase images of rGO film, obtained by tapping mode atomic force microscopy (AFM) are shown in Figure 6c and Figure 6d. The film with peculiar corrugations showed roughness of 5.7 nm.

The C(1s) and O(1s) XPS spectra obtained from the same rGO film are shown in Figures 7a and 7b. The deconvoluted C(1s) XPS peak centered at binding energy of 284.5 eV is assigned to C-C (sp²) in graphite.³³ The component at 285.6 eV is assigned to C atoms in C-C (sp³) at defects; the peak at 286.5 eV is attributed to epoxide (C-O-C) and C-OH groups;³⁴ and the line at 288.0 eV is assigned to (-C=O) of quinone groups on the film surface (Figure 7a).^{21,35} The summary of assignments and group % is shown in Table 2. These percentages should be considered as only a guide for the discussion because the best fitting of the XPS lines lead to large peaks which are superimposed, as for instance, the peaks at 284.5 eV and 285.6 eV.

The deconvolution of O (1s) peaks gives complementary qualitative information about the nature of the GO surface. The peak at 530.6 eV corresponds to the oxygen bonded to aromatic carbon atoms as quinone groups;³⁴ and the large peak at ca. 532.0 eV can be attributed to carbonyl oxygen atoms in esters, as well as oxygen atoms in hydroxyls or

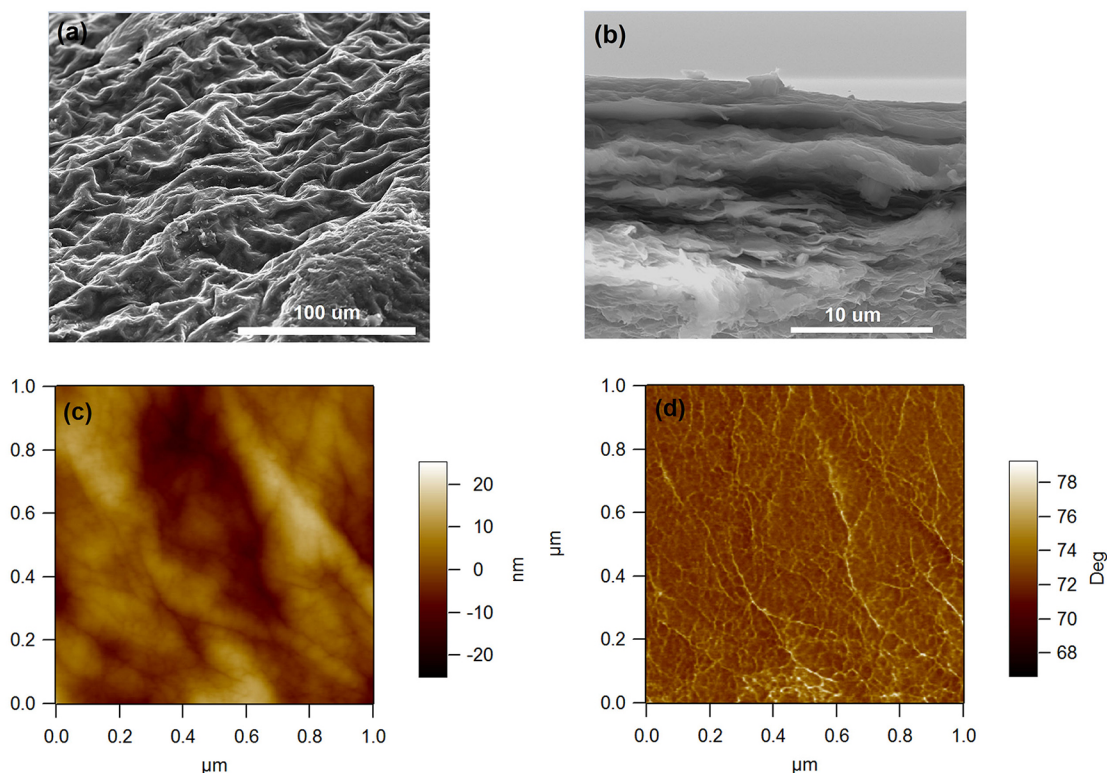


Figure 6. SEM images of the rGO film: (a) top and (b) cross-sectional views; (c) AFM morphology and (d) phase image of rGO film.

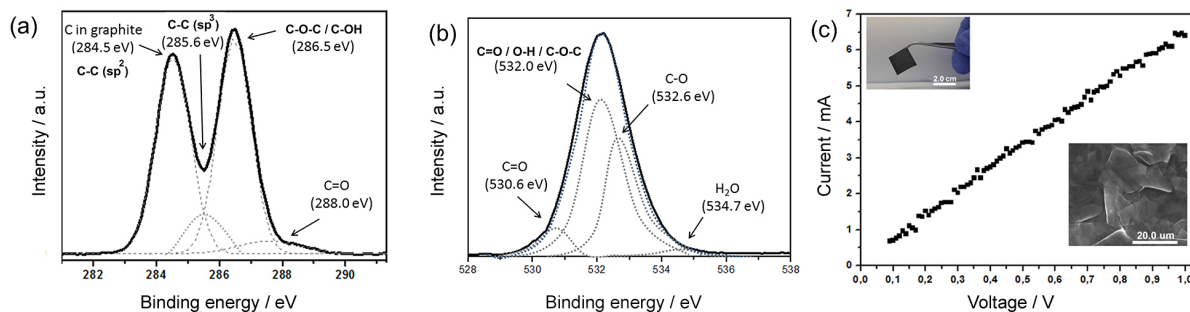


Figure 7. (a) C(1s) and (b) O(1s) XPS spectra of the rGO film; (c) Electrical measurement of a rGO film deposited onto a Si/SiO₂ substrate.

Table 2. XPS results obtained from fitting of C(1s) and O(1s) spectra

Binding Energy / eV		Bond and functional group		Group / %	
C (1s)	O (1s)	C (1s)	O (1s)	C (1s)	O (1s)
284.5	530.6	C–C (sp ²)	C=O	40.2	7.6
285.6	532.0	C–C (sp ³)	C=O/O–H/C–O–C ^a	8.5	52.1
286.5	532.6	C–O–C/C–OH	C–O	47.2	38.4
288.0	534.7	C=O	H ₂ O	4.1	1.9

^aCarbonyl oxygen atoms in esters, as well as oxygen atoms in hydroxyls or ethers show signals in this region.

ethers; the peak at 532.6 eV may correspond to ether oxygen atoms in esters; and at 534.7 eV a line can be associated to the oxygen atoms in the carboxyl groups or in H–O–H.³⁵ The fitting lines at 532.0 eV and 532.6 eV are strongly superimposed and this preclude any specific conclusion about the content of oxygenated functional group content in the GO. The total atomic percentage of C and O observed by XPS is 69% and 31%, respectively. These results are in agreement with the percentage of oxygenated groups determined by TGA measurements.

Table 2 lists the XPS peaks attributed to C–C and C–O bonds and the group percentages in the rGO film structure.

Figure 7c presents the current-voltage plot of this rGO film annealed at 110 °C deposited on a Si/SiO₂ substrate that exhibits a resistivity of $1.35 \times 10^{-3} \Omega \text{ m}$ and a corresponding electrical conductivity of $7.36 \times 10^2 \text{ S m}^{-1}$. The relatively high conductivity of the film after it was annealed at 110 °C overnight clearly indicates good restoration of the π -conjugated system at low temperatures, induced by the deoxygenation and dehydration process. Probably, during the washing and centrifugation process of GO the more defective and oxidative sheets were eliminated and the large sheets with low defects were selected to form the rGO film as evidenced by AFM and TEM images. Some authors^{36–39} have described the preparation of reduced GO powder and film using hydrazine and/or annealing treatment and observed conductivity values that were lower or similar than the conductivity of the rGO film prepared here. Li *et al.*⁴⁰ have prepared GO sheets by Hummers method and rGO film by filtration and subsequent thermal annealing at 750 °C

under argon atmosphere for 2 h. The authors found a higher electrical conductivity of $1.076 \times 10^4 \text{ S m}^{-1}$ to rGO film with the same thickness (30 μm) as the rGO film prepared in this work. When Bi *et al.*⁴¹ synthesized graphene sheets by chemical vapor deposition (CVD) and graphene film with thickness of about 25 μm was reached the outstanding value of $1.097 \times 10^5 \text{ S m}^{-1}$ due to low structural defects in graphene sheets. It is well known that the electrical conductivity of rGO films is dependent on characteristics as amount of defects, annealing temperature, reduction atmosphere, film thickness and oxidation residual. In this work the rGO film was submitted to low annealing temperature for longer than other studies cited above showing an unexpected conductivity value which probably can improve with increasing annealing temperature. This result demonstrates the potential of our rGO sheets to be uses in electrical devices.

Conclusions

In this work, rGO films were synthesized using a microwave-assisted acid technique, demonstrating that microwaves are a versatile form of radiation that facilitates chemical reactions in the carbon structure. The oxygenated groups present on the GO surface: carboxyl, epoxy, hydroxyl and carbonyl groups, were identified by UV-Vis, XPS and FTIR techniques. The rGO film deposited onto Si/SiO₂ substrates and dried at 110 °C overnight exhibited an inter-sheet spacing of 0.70 nm and an electrical conductivity of $7.36 \times 10^2 \text{ S m}^{-1}$, confirming the good restoration of the π -conjugated system. Wrinkled 2D GO with 5 to 9 layers,

as determined by AFM, SEM and TEM images, exhibited predominantly negative charges and good stability in water in the pH range from 4 to 12. The method described here is promising for the preparation of GO nanosheets that aid in the understanding of the physics and chemistry of graphene, enabling their use in various engineering applications.

Acknowledgments

This work was financially supported by The Brazilian National Council for Technological and Scientific Development (CNPq) and Petrobras. The authors acknowledge the Pró-Reitoria de Pesquisa of Universidade Federal de Minas Gerais and the Microscopy Center of Universidade Federal de Minas Gerais for the SEM and AFM images.

References

- Novoselov, K. S.; Geim, A. K.; Morozov, S. V.; Jiang, D.; Zhang, Y.; Dubonos, S. V.; Grigorieva, I. V.; Firsov, A. A.; *Science* **2004**, *306*, 666.
- Park, S.; Ruoff, R. S.; *Nat. Nanotechnol.* **2009**, *4*, 217.
- Brodie, B. C.; *Ann. Chim. Phys.* **1860**, *59*, 466.
- Staudenmaier, L.; *Ber. Deut. Chem. Ges.* **1898**, *31*, 1481.
- Hummers, W. S.; Offeman, R. E.; *J. Am. Chem. Soc.* **1958**, *80*, 1339.
- Wang, G.; Wang, B.; Park, J.; Yang, J.; Shen, X.; Yao, J.; *Carbon* **2009**, *47*, 68.
- Sathyamoorthi, S.; Suryanarayanan, V.; Velayutham, D.; *J. Solid State Electrochem.* **2014**, *18*, 2789.
- Sridhar, V.; Jeon, J.-H.; Oh, I.-K.; *Carbon* **2010**, *48*, 2953.
- Wei, T.; Fan, Z.; Luo, G.; Zheng, C.; Xie, D.; *Carbon* **2009**, *47*, 337.
- Zhu, Y.; Murali, S.; Stoller, M. D.; Velamakanni, A.; Piner, R. D.; Ruoff, R. S.; *Carbon* **2010**, *48*, 2118.
- Clauss, A.; Plass, R.; Boehm, H. P.; Hofmann, U.; *Z. Anorg. Allg. Chem.* **1957**, *291*, 205.
- Lerf, A.; He, H. Y.; Forster, M.; Klinowski, J.; *J. Phys. Chem. B* **1998**, *102*, 4477.
- Scholz, W.; Boehm, H. P.; *Z. Anorg. Allg. Chem.* **1969**, *369*, 327.
- Szabo, T.; Berkesi, O.; Forgo, P.; Josepovits, K.; Sanakis, Y.; Petridis, D.; Dekany, I.; *Chem. Mater.* **2006**, *18*, 2740.
- Dimiev, A. M.; Alemany, L. B.; Tour, J. M.; *ACS Nano* **2013**, *7*, 576.
- Erickson, K.; Erni, R.; Lee, Z.; Alem, N.; Gannett, W.; Zettl, A.; *Adv. Mater.* **2010**, *22*, 4467.
- Dikin, D. A.; Stankovich, S.; Zimney, E. J.; Piner, R. D.; Dommett, G. H. B.; Evmenenko, G.; Nguyen, S. T.; Ruoff, R. S.; *Nature* **2007**, *448*, 457.
- Singh, V.; Joung, D.; Zhai, L.; Das, S.; Khondaker, S. I.; Seal, S.; *Prog. Mater. Sci.* **2011**, *56*, 1178.
- Jeon, G. W.; Jeong, Y. G.; *J. Mater. Sci.* **2013**, *48*, 4041.
- Shao, G.; Lu, Y.; Wu, F.; Yang, C.; Zeng, F.; Wu, Q.; *J. Mater. Sci.* **2012**, *47*, 4400.
- Wan, L.; Liu, P.; Zhang, T.; Duan, Y.; Zhang, J.; *J. Mater. Sci.* **2014**, *49*, 4989.
- Becerril, H. A.; Mao, J.; Liu, Z.; Stoltenberg, R. M.; Bao, Z.; Chen, Y.; *ACS Nano* **2008**, *2*, 463.
- Park, S.; Lee, K.-S.; Bozoklu, G.; Cai, W.; Nguyen, S. T.; Ruoff, R. S.; *ACS Nano* **2008**, *2*, 572.
- Leng, X.; Xiong, X.; Zou, J.; *Trans. Nonferrous Met. Soc. China* **2014**, *24*, 177.
- Xin, G.; Hwang, W.; Kim, N.; Cho, S. M.; Chae, H.; *Nanotechnology* **2010**, *21*, 405201.
- Dimiev, A.; Kosynkin, D. V.; Alemany, L. B.; Chaguine, P.; Tour, J. M.; *J. Am. Chem. Soc.* **2012**, *134*, 2815.
- Li, D.; Mueller, M. B.; Gilje, S.; Kaner, R. B.; Wallace, G. G.; *Nat. Nanotechnol.* **2008**, *3*, 101.
- Shang, J.; Ma, L.; Li, J.; Ai, W.; Yu, T.; Gurzadyan, G. G.; *Sci. Rep.* **2012**, *2*, 1.
- ASTM D4187-82: *Zeta Potential of Colloids in Water and Waste Water, Standard*, Philadelphia, 1985.
- Wang, X.; Bai, H.; Shi, G.; *J. Am. Chem. Soc.* **2011**, *133*, 6338.
- Silva, W. M.; Ribeiro, H.; Seara, L. M.; Calado, H. D. R.; Ferlauto, A. S.; Paniago, R. M.; Leite, C. F.; Silva, G. G.; *J. Braz. Chem. Soc.* **2012**, *23*, 1078.
- Hsieh, C.-T.; Chen, W.-Y.; *Surf. Coat. Technol.* **2011**, *205*, 4554.
- Teng, C.; Ma, C. M.; Lu, C.; Yang, S.; Lee, S.; Hsiao, M.; Yen, M.; Chiou, K.; Lee, T.; *Carbon* **2011**, *9*, 3.
- Ganguly, A.; Sharma, S.; Papakonstantinou, P.; Hamilton, J. P.; *J. Phys. Chem. C* **2011**, *115*, 17009.
- Chiang, Y.; Lin, W.; Chang, Y.; *Appl. Surf. Sci.* **2011**, *257*, 2401.
- Stankovich, S.; Dikin, D. A.; Piner, R. D.; Kohlhaas, K. A.; Kleinhammes, A.; Jia, Y.; Wu, Y.; Nguyen, S. T.; Ruoff, R. S.; *Carbon* **2007**, *45*, 1558.
- Smirnov, V. A.; Denisov, N. N.; Ukshe, A. E.; Shulga, Y. M.; *Chem. Phys. Lett.* **2013**, *583*, 155.
- Chen, H.; Muller, M. B.; Gilmore, K. J.; Wallace, G. G.; Li, D.; *Adv. Mater.* **2008**, *20*, 3557.
- Sun, H. B.; Yang, J.; Zhou, Y. Z.; Zhao, N.; Li, D.; *Mater. Technol. Adv. Perform. Mater.* **2014**, *29*, 14.
- Li, P.; Yao, H.; Wong, M.; Sugiyama, H.; Zhang, X.; Sue, H.-J.; *J. Mater. Sci.* **2014**, *49*, 380.
- Bi, H.; Chen, J.; Zhao, W.; Sun, S.; Tang, Y.; Lin, T.; Huang, F.; Zhou, X.; Xied, X.; Jiang, M.; *RSC Adv.* **2013**, *3*, 8454.

Submitted: November 14, 2014

Published online: March 13, 2015